Journal of Biomolecular Structure and Dynamics

ISSN: (Print) (Online) Journal homepage: www.tandfonline.com/journals/tbsd20

Evaluation of the impact of two C5 genetic variants on C5-eculizumab complex stability at the molecular level

Vanda P. Peixoto, Cristina Prudêncio, Mónica Vieira & Sérgio F. Sousa

To cite this article: Vanda P. Peixoto, Cristina Prudêncio, Mónica Vieira & Sérgio F. Sousa (26 Mar 2024): Evaluation of the impact of two C5 genetic variants on C5-eculizumab complex stability at the molecular level, Journal of Biomolecular Structure and Dynamics, DOI: 10.1080/07391102.2024.2331091

To link to this article: https://doi.org/10.1080/07391102.2024.2331091

JOURNAL OF BIOMOLECULAR STRUCTURE AND DYNAMICS
https://doi.org/10.1080/07391102.2024.2331091

Evaluation of the impact of two C5 genetic variants on C5-eculizumab complex stability at the molecular level

Vanda P. Peixoto[a,b,c], Cristina Prudêncio[a,b,d], Mónica Vieira[a,b,d] and Sérgio F. Sousa[c]

[a]Chemical and Biomolecular Sciences, School of Health, Polytechnic Institute of Porto, Porto, Portugal; [b]Center for Translational Health and Medical Biotechnology Research (TBIO), Polytechnic Institute of Porto, Porto, Portugal; [c]LAQV/REQUIMTE, BioSIM - Departamento de Biomedicina, Faculdade de Medicina, Universidade do Porto, Porto, Portugal; [d]Institute for Research and Innovation in Health (i3S), University of Porto, Porto, Portugal

Communicated by Ramaswamy H. Sarma

ABSTRACT

Complement C5 is the target of the monoclonal antibody eculizumab, used in complement dysregulating disorders, like the rare disease Paroxysmal Nocturnal Hemoglobinuria (PNH). PNH is an acquired hematopoietic stem cell condition characterized by aberrant destruction of erythrocytes, chronic hemolytic anemia, and thromboembolism propensity. C5 is a protein component of the complement system which is part of the immune system of the body and plays a prominent role in the destruction of red blood cells, misidentifying them as a threat. This work describes the application of molecular dynamics simulations to the study of the underlying interactions between complement C5 and eculizumab. This study also reveals the importance of single nucleotide polymorphisms on C5 protein concerning the effective inhibition of the mAB, involving the mechanistic events taking place at the interface spots of the complex. The predicted conformational change in the C5 Arg^{885}/His/Cys mutation has implications on the protein's interaction with eculizumab, compromising their compatibility. The acquired insights into the conformational changes, dynamics, flexibility, and interactions shed light on the knowledge of the function of this biomolecule providing answers about the poor response to the treatment in PNH patient carriers of the mutations. By investigating the intricate dynamics, significant connections between C5 and eculizumab can be uncovered. Such insights may aid in the creation of novel compounds or lead to the enhancement of eculizumab's efficacy.

ARTICLE HISTORY
Received 29 November 2023
Accepted 11 March 2024

KEYWORDS
Computational simulation; eculizumab; complement C5; genetic polymorphisms; structural analysis

Introduction

Paroxysmal nocturnal hemoglobinuria (PNH) is an acquired hematological disease that arises from a somatic mutation. The mutation primarily occurs in hematopoietic stem cells in the bone marrow. The disease is originated by phosphatidylinositol-*N*-acetylglucosaminyltransferase subunit A gene (PIG-A) mutation and consequent loss of function. PIG-A is a X-linked gene required for the biosynthesis of glycosylphosphatidylinositol (GPI), that anchors important proteins on membrane blood cells surface (Bessler et al., 1994; Brodsky, 2014; Takeda et al., 1993).

CD55 and CD59 are GPI-anchored proteins of the surface of red blood cells (RBCs). As complement-regulatory proteins, they can inhibit complement system attack, protecting cells from its destruction. CD55 blocks C3 convertase, while CD59 blocks membrane attack complex (MAC) (Figure 1). The absence of GPI molecule leads to the absence of these proteins on RBCs surface. These RBCs are hence recognized as damaged, leading to hemolysis mediated by the complement system, with release of the hemoglobin into the bloodstream (Schmidt et al., 2022).

The complement system is part of the innate immunity system that includes a set of plasma and serum proteins. Complement activation can be reached either by the classical, alternative and lectin pathways. C3 convertases cleave C3 in C3a and C3b which leads to formation of C5 convertase. C5 is cleaved into C5a and C5b. C5b activates terminal cascade C6, C7, C8 and C9 forming C5b-9 complex MAC, that ultimately leads to cell destruction (Bektas et al., 2020). From the initial PIG-A mutation, a group of blood cells carrying the same genetic alteration emerges. These cells are called PNH clones and progressively establish dominance within the bone marrow, resulting in the distinctive characteristics associated with PNH (Brodsky, 2009; Heeney et al., 2003).

PNH is a life-threatening disease. Besides hemolytic anemia it can be related to bone marrow aplasia and thromboembolism (TE). TE is the most feared outcome, contributing to morbidity and mortality. In a relatively recent study, 29% of PNH patients without treatment have 10 years span of life after diagnosis (Fu et al., 2020).

The first approved treatment for PNH was the humanized monoclonal antibody (mAB), eculizumab. Eculizumab inhibits terminal complement factor C5, preventing its cleavage,

CONTACT Vanda P Peixoto vpp@ess.ipp.pt Chemical and Biomolecular Sciences, School of Health, Polytechnic Institute of Porto, Porto, Portugal; Sérgio F Sousa sergiofsousa@med.up.pt LAQV/REQUIMTE, BioSIM - Departamento de Biomedicina, Faculdade de Medicina, Universidade do Porto, Porto, Portugal.

Supplemental data for this article can be accessed online at https://doi.org/10.1080/07391102.2024.2331091.

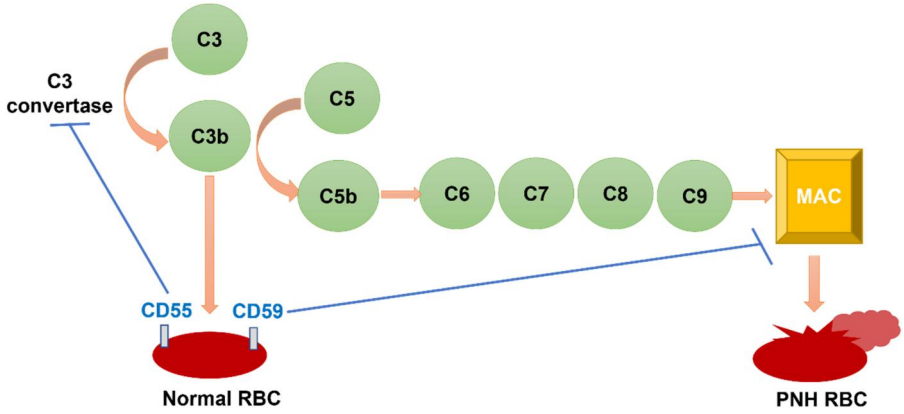

Figure 1. Protection of GPI-anchored proteins CD55 and CD59 of red blood cells from complement system.

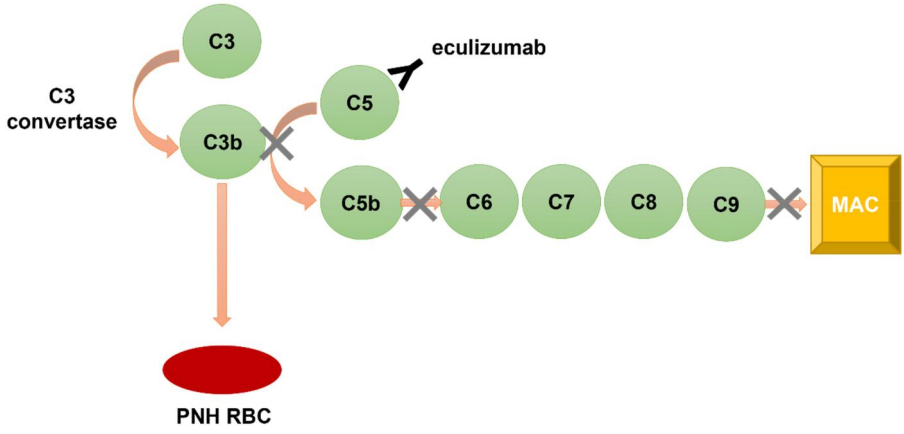

Figure 2. Eculizumab inhibition of C5 on terminal pathway of complement cascade.

inhibiting complement-mediated hemolysis (Schrezenmeier & Höchsmann, 2009; Figure 2). Response to anti-complement therapies, like eculizumab, lead to hemoglobin stabilization in most patients and represented a drastic change in the improvement of quality of life, life expectancy and in the control of symptoms and of clinical levels of patients with PNH (Brodsky et al., 2008; Hillmen et al., 2006, 2013).

PNH patients treated with eculizumab can have different responses to treatment. Most patients achieve transfusion independence. However, some may still require transfusions, and although hemoglobin levels can remain steady, they may still experience anemia (Risitano et al., 2009, 2019).

In some cases, eculizumab anti-complement therapy is inefficient. Activation of terminal pathway complement proteins can exacerbate in some health conditions, like severe infections, and thus, eculizumab is not sufficient to prevent intravascular hemolysis (Harder et al., 2019).

Single nucleotide variants (SNVs) are a prevalent form of genetic variation in the human population. The majority of these SNVs are benign and are referred to as single nucleotide polymorphisms (SNPs). SNPs play a significant role in genetic variability and can be linked to physical traits, susceptibility to diseases, and how individuals respond to treatments (Katsonis et al., 2014).

In a study with Japanese patients with PNH, a small portion (3.2%) of the patients showed poor response to eculizumab. Genetic variants in complement C5 were searched and it was found a single missense heterozygous mutation, c.2654 G > A, which expresses the p.Arg^{885}His variant. Another Asian descendent patient had shown a similar mutation, c.2653 > T, which expresses p.Arg^{885}Cys polymorphism (Nishimura et al., 2014).

A crystal structure of the complex between C5 and a Fab fragment with V region with the same sequence as eculizumab, demonstrated the importance of the interaction at this site. This mutation is located on the binding region of eculizumab to C5, so the resulting complex is thought to lose stability, resulting in weaker inhibition by the antibody (Schatz-Jakobsen et al., 2016).

Molecular dynamics (MD) simulations can be used to analyze structures and predict the molecular behavior of biological systems (Elzaiat et al., 2020; Mahtarin et al., 2022; Mohamed et al., 2020; Muthukumar, 2023). In this work, MD studies were performed to analyze from a dynamic perspective the recognition of eculizumab by C5 and to determine the molecular determinants for this interaction. The study was then extended to understand the structural and dynamic impact of p.Arg^{885}His/Cys variants in the stability of C5-eculizumab complex.

Methods

Parameters for the analysis of complement C5 in complex with eculizumab

The structure of the *homo sapiens* complement C5-eculizumab complex was obtained from the Protein Data Bank (Berman et al., 2000), entry 5I5K (Schatz-Jakobsen et al.,

2016) corresponding to its Cryo-EM structure with a 4.2 Å resolution.

This structure was aligned with the complement C5 model available at the alpha fold structural database (Jumper et al., 2021; Varadi et al., 2022). A full model was built starting from the 5I5K experimental structure with the missing amino acid residues modelled from the alpha fold structural database model. The protonation state of all amino acid residues at pH 7.0 was predicted using the PlayMolecule web server (Martínez-Rosell et al., 2017).

The preparation of the system involved the use of the AMBER20 software package and Xleap. The system was described using the ff14SB force field (Maier et al., 2015). Using the LEAP module of AMBER software, charges on the complex system were neutralized through the addition of counter-ions (Cl^-) and the system was placed in a TIP3P water model box with a minimum distance of at least of 12 Å between the protein surface and the border of the box, treated with periodic boundary conditions.

The 3D figure structures were prepared with VMD (Humphrey et al., 1996).

Molecular dynamics simulations (MD) analyses of complement C5 complex with eculizumab

For the analyses of the p.Arg^{885}His and the p.Arg^{885}Cys variants, the wild-type complex was modeled with the mutagenesis feature in Pymol 1.7.2.1 software, using the Dunbrack rotamer libraries (Shapovalov & Dunbrack, 2011; Weiser et al., 1999). The dominant conformer predicted an initial amino acid conformation for each mutated structure. Conformers exhibiting clashes with the other residues of the protein were excluded. The computational mutagenesis protocol has been previously used with good results in other studies (Ferreira et al., 2017; Lapaillerie et al., 2022; Magalhães et al., 2022; Quelhas et al., 2021; Serrano et al., 2021).

The solvation and neutralization protocol described were applied in both the wild-type system and the mutant systems. The three systems were subjected to four consecutive energy minimization stages to remove clashes before the molecular dynamics (MD) simulation. In these four stages, the minimization procedure was applied to the following atoms of the system: (i) water molecules (2500 steps); (ii) hydrogen atoms (2500 steps); (iii) side chains of the amino acid residues (2500 steps); (iv) full system (10,000 steps). The energy minimized systems were then submitted to a two stages MD equilibration protocol: (i) the systems were gradually heated to 310.15 K using a Langevin thermostat at a constant volume (NVT ensemble) (50 ps); (ii) the density of the systems was equilibrated at 310.15 K (50 ps).

MD simulation runs were performed for 3 replicas of 300 ns for the wild-type complex, and the 2 mutants, representing a total of 2700 ns of simulation ($3 \times 3 \times 300$ ns). These were performed in an NPT ensemble at constant temperature (310.15 K, Langevin thermostat) and pressure (1 bar, Berendsen barostat), with periodic boundary conditions, with an integration time step of 2.0 fs using the SHAKE algorithm to constrain all covalent bonds involving hydrogen atoms. A 10 Å cut-off for nonbonded interactions was used during the entire molecular simulation procedure. Coordinates were saved at each 10 ps. Final trajectories were analyzed in terms of backbone root-mean-square deviation (RMSd), and root-mean-square fluctuation (RMSF).

Molecular mechanics/generalized born surface area (MM-GBSA)

The MM-GBSA method (Miller et al., 2012) was employed to predict the C5-eculizumab complex binding free energy. The contribution of all amino acid residues for each of these binding free energies was estimated applying the energy decomposition method. From each MD simulations trajectory, a total of 300 conformations taken from the last 300 ns of simulation were considered for each MM-GBSA calculation.

According to the MM-GBSA method the binding free energy can be decomposed as:

$$\Delta G_{bind} = G_{complex} - (G_{C5} + G_{eculizumab})$$

The internal energy change (ΔE_{int}) is canceled because the structures of complex, C5, and eculizumab are extracted from the same trajectory.

$$\Delta E_{gas} = \Delta E_{int} + \Delta E_{ELE} + \Delta E_{VDW}$$
$$\Delta G_{sol} = \Delta G_{GB} + \Delta G_{Surf}$$

The gas-phase interaction energy (ΔE_{gas}) between the components is calculated as the sum of electrostatic (ΔE_{ELE}) and van der Waals (ΔE_{VDW}) interaction energies. The solvation free energy (ΔG_{sol}) is written as the sum of the polar and the non-polar energy terms. The polar solvation energy (ΔG_{GB}) is calculated by using the Generalized-born (GB) model, proposed by Onufriev, Bashford and Case (Onufriev et al., 2004). The non-polar contribution is calculated based on the solvent-accessible surface area (ΔG_{Surf}), calculated with the LCPO method (Weiser et al., 1999). The binding free energy (ΔG_{bind}) is written as the sum of the gas-phase interaction energy and solvation free energy. The ΔG_{bind} values reported in this study exclude the entropy contribution, as it is known to introduce additional errors into the comparison data. Association free energies were calculated using this protocol in several other different biomolecular studies, with good results (Martins et al., 2021; Pereira et al., 2022; Pina et al., 2022).

Results and discussion

Mapping of the C5-eculizumab interface

To understand at the molecular level the structural determinants for C5-eculizumab binding in the wt protein, the MM-GBSA method was applied. In particular, a per-residue decomposition analysis of the complexation free energy was performed. The results show the amino acid contributing the most to the stabilization of the C5-eculizumab.

The amino acids with the largest contribution for the formation C5-eculizumab complex and to its stability are Arg^{885}, Trp^{917}, Gln^{854}, Phe^{918} and Glu^{915}. All these residues have a

free energy contribution of between −1.7 ± 1.1 and −8.8 ± 0.9 kcal/mol to the complex binding free energy (hot spots, the more negative, the highest the contribution to complex stabilization; Table 1).

The position of these residues in the 3D structure of the complex is highlighted in Figure 3.

Table 1. Energetic contribution of most important residues as estimated by the MM-GBSA method.

Residues	$\Delta G_{binding}$ (kcal/mol)
GLN^{854}	−3.5 ± 1.5
ARG^{885}	−8.8 ± 0.9
GLU^{915}	−1.7 ± 1.1
TRP^{917}	−7.4 ± 0.8
PHE^{918}	−1.8 ± 0.3

Arg^{885} is the highest contributor to the complexation free energy (−8.8 ± 0.9 kcal/mol), followed by Trp^{917} (−7.4 ± 0.8 kcal/mol). These results confirm these two amino acid residues as the major participants for eculizumab interaction with C5. Gln^{854}, Glu^{915} and Phe^{918} have a contribution to the complex free energy of −3.5 ± 1.5, −1.7 ± 1.1 and −1.8 ± 0.3 kcal/mol, respectively. The known eculizumab conformational epitope is represented in Figure 4A and is composed of a β-strand (884–890) and a β-hairpin (913–922) containing these main residues. These residues are part of the C5 MG7 domain, which is the domain that interacts with eculizumab (Jore et al., 2016).

Our silico approach corroborates some aspects related to the complex interaction, mentioned before in other analyses (Brachet et al., 2016; Schatz-Jakobsen et al., 2016):

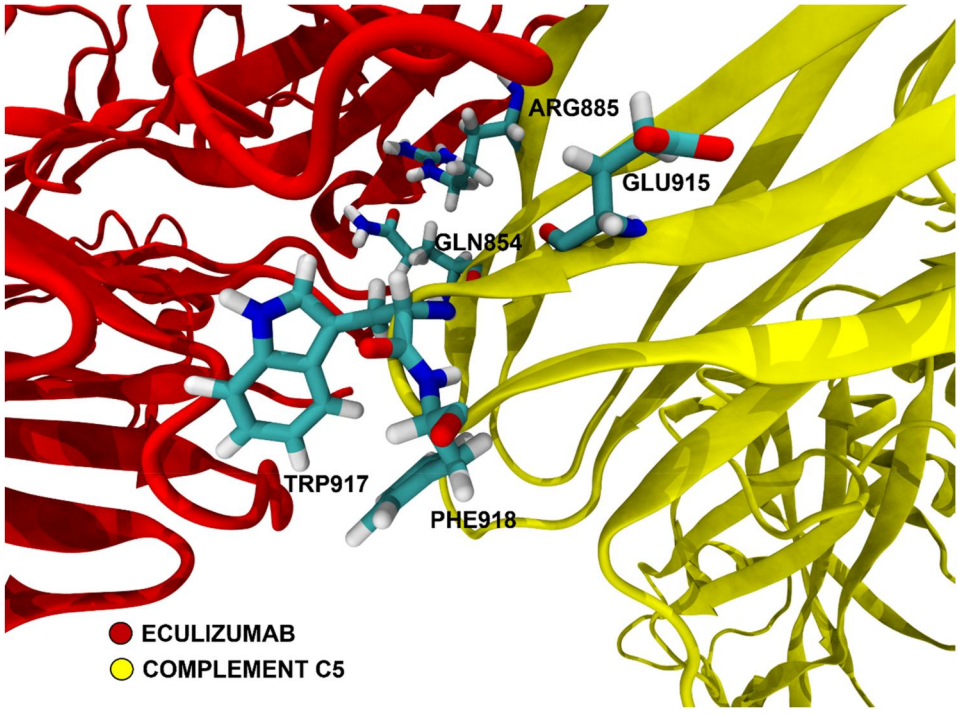

Figure 3. Visual molecular dynamics (VMD) representation of the alignment of the representative structure of the C5-eculizumab complex. The five amino acids with major energetic contribution are highlighted.

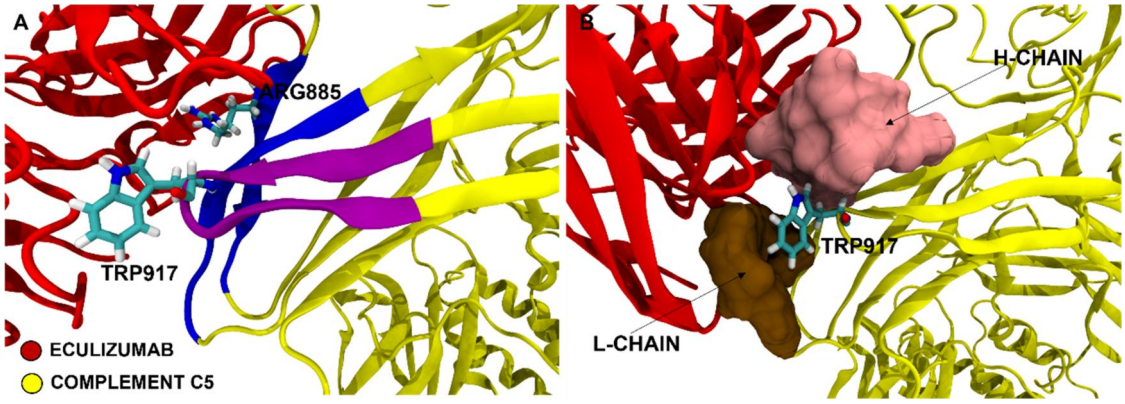

Figure 4. Visual molecular dynamics (VMD) representation of the alignment of the representative structure of the C5-eculizumab complex. (A) Eculizumab epitope. (B) Interaction of C5 with a binding pocket region (101–107 residues of H-CDR3, 30–32 residues of L-CDR1 and 92 residue of L-CDR3) formed on the surface of eculizumab.

The β-strand contains the key residue Arg^{885} which engages with the H chain of eculizumab (H-CDR3).

Another β-strand (851–858) and the previous β-strand are held by a disulfide bridge (856–883).

Tpr^{917} is part of the hairpin formed between residues Ser^{913} and Ile^{922} and "fits" inside a binding pocket region that forms in the eculizumab surface (defined by residues 101–107 of the H chain, and 30–32 and 92 of the L chain) (Figure 4B). Tpr^{917} interacts with the phenol group of Tyr^{99}.

Eculizumab interacts with these specific peptide regions of C5, acting as a competitor of C5 convertases. C5 convertase cleaves the scissile bond between Arg^{751} and Leu^{752}, located distal to eculizumab epitope. Eculizumab can sterically block the access to convertases, interacting with the previous residues mentioned above.

Mapping the structural and dynamic effect of mutants: (p.Arg^{885}His and p.Arg^{885}Cys interface)

To further analyze the importance of Arg^{885} in the formation of the C5-Eculizumab complex and to understand the effect of mutations on this position by histidine or cysteine, as in the reported genetic variants for complement C5, a comparative analysis of the structure, dynamics and associated energetics of the wild-type, p.Arg^{885}His and p.Arg^{885}Cys variants was performed.

Table 2 presents the average C5-Eculizumab complexation free energies determined for the three systems and corresponding non-polar and polar contribution. As expected, an analysis of Table 2 shows that both mutations lead to a less stable C5-Eculizumab complex than in the wild-type C5 system.

In p.Arg^{885}His the arginine alteration to histidine decreases the binding affinity of eculizumab, resulting in an increase in ΔG_{bind} of 17.4 kcal/mol, from −69.8 to −52.4 kcal/mol. For p.Arg^{885}Cys, the ΔG_{bind} difference was also significant, with an increase of +9.4 kcal/mol, from −69.8 to −60.4 kcal/mol.

An analysis of the energetic components to the complexation free energy shows that the non-polar contribution to the eculizumab binding free energy in the mutated variants decreases when compared to the WT, representing an unfavorable energy change for the stability of the complex arising from a decrease in hydrophobic interactions. In addition, the polar contribution to the eculizumab binding free energy for the mutated variants increases, becoming more positive, also representing an unfavorable energy change for the polymorphic variants.

Figure 5 shows the energetic contribution of the most important amino acid residues to the formation of the C5-eculizumab in the WT and Arg^{885}His and p.Arg^{885}Cys variants.

As expected, the biggest difference is observed for position 885, where the different variants differ in amino acid. As mentioned before, the average binding energy of the amino acid Arg^{885} is −8.8 kcal/mol for the WT. For the histidine and the cysteine mutation, this value changes to −2.9 and −2.9, respectively. The non-polar contribution is more favorable for histidine variant, but less favorable for cysteine mutation (−5.6 in wt vs. −6.1 and −3.4 kcal/mol for the His and Cys variants, respectively). The polar contribution (−3.2 in wt vs. 3.2 and 0.5 kcal/mol for the His and Cys variants, respectively) also shows less favorable contribution for polymorphic residues (Table 3).

This effect arises to a great extent from the elimination of the salt-bridge between Arg^{885} of C5 and Glu^{50} of the H chain of eculizumab. Variants p.Arg^{885}His and p.Arg^{885}Cys both lose this key interaction, weakening the eculizumab binding ability to C5.

Table 2. Energetic contribution of all system.

System	ΔG_{bind} (kcal/mol)	Non-polar contribution (kcal/mol)	Polar contribution (kcal/mol)
WT	−69.8 ± 2.9	−119.5 ± 9.8	49.6 ± 7.1
p.Arg^{885}His	−52.4 ± 5.7	−110.9 ± 12.8	58.5 ± 7.6
p.Arg^{885}Cys	−60.4 ± 13.4	−112.6 ± 17.3	52.2 ± 5.9

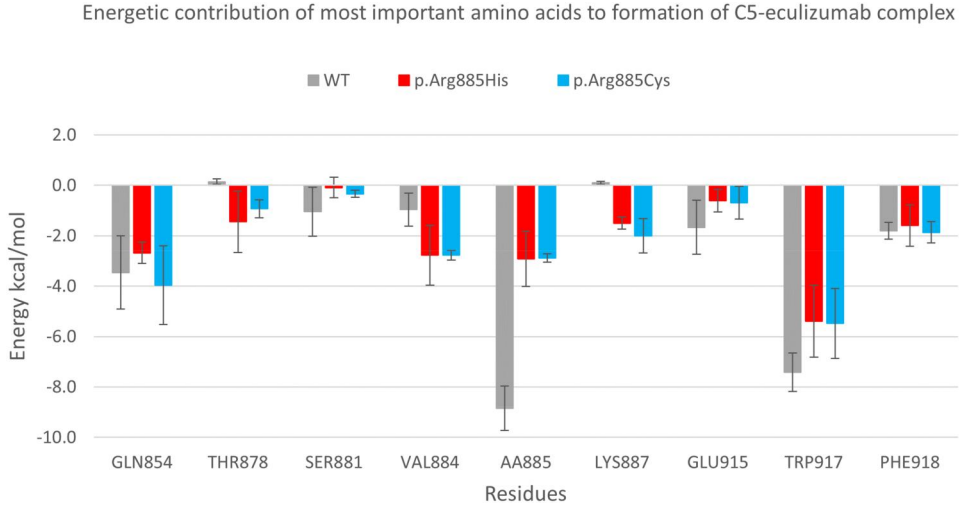

Figure 5. Energetic contribution of most important amino acids to formation of C5-eculizumab.

Figure 6 shows the difference in C5-eculizumab interaction for position 885 in the three systems, as observed from the average structure of the dominant conformer obtained for each simulation. Average bond distance shows significant alterations between the three systems (4.0 ± 0.1 in wt vs. 5.8 ± 1.3 and 8.9 ± 1.3 Å for the His and Cys variants, respectively).

The average binding energy of Trp^{917} is −7.4 kcal/mol in its natural state. However, when Arg^{885} is replaced with Histidine or Cysteine, this energy value goes to −5.4 and −5.5 kcal/mol, respectively.

Regarding the non-polar component, both variants have less favorable energy values, yielding −8.3 and −8.1 kcal/mol (His and Cys, respectively), compared to the wild-type's −10.5 kcal/mol. The polar component (3.1 in wt vs. 2.9 and 2.6 kcal/mol for the His and Cys variants, respectively) does not represent a high variation.

The neighbor residue Phe^{918}, did not significantly alter the energy input on polymorphic variants when compared with wild-type (−1.8 in wt vs. −1.6 and −1.9 kcal/mol for the His and Cys variants, respectively).

Other amino acids in the vicinity of these mutations, exhibit alterations that prove to be unfavorable for the binding to C5, as they have less negative values in nonpolar contribution and higher values in polar contribution (Glu^{915} and Ser^{881}).

However, the residues Val^{884}, Thr^{878} and Lys^{887} appear to attempt to compensate for the destabilization of the complex in both mutated species, showing an increased contribution (more negative) when in comparison with the wild-type. The non-polar energetic contribution was favorable to the bond connection of the complex for p.Arg^{885}His and p.Arg^{885}Cys variants, playing a predominant role.

Table 3. Energetic contribution of most important amino acids of C5-eculizumab complex in wild-type and in p.Arg^{885}His/p.Arg^{885}Cys mutants.

	$\Delta G_{binding}$ (kcal/mol)			Non-polar contribution (kcal/mol)			Polar contribution (kcal/mol)		
Residue	WT	p.Arg^{885}His	p.Arg^{885}Cys	WT	p.Arg^{885}His	p.Arg^{885}Cys	WT	p.Arg^{885}His	p.Arg^{885}Cys
GLN854	**−3.5 ± 1.5**	**−2.7 ± 0.4**	**−4.0 ± 1.6**	**−5.6 ± 0.6**	**−4.7 ± 0.4**	**−5.4 ± 1.0**	**2.1 ± 1.1**	**2.0 ± 0.6**	**1.5 ± 0.6**
THR878	0.1 ± 0.1	−1.4 ± 1.2	−0.9 ± 0.4	−0.3 ± 0.2	−1.5 ± 0.8	−1.2 ± 0.1	0.4 ± 0.3	0.0 ± 0.5	0.2 ± 0.5
SER881	−1.0 ± 1.0	−0.1 ± 0.4	−0.3 ± 0.1	−1.4 ± 1.0	−0.5 ± 0.5	−0.8 ± 0.1	0.4 ± 0.0	0.4 ± 0.1	0.4 ± 0.1
VAL884	−1.0 ± 0.7	−2.8 ± 1.2	−2.8 ± 0.2	−1.4 ± 0.8	−3.2 ± 1.1	−3.4 ± 0.3	0.5 ± 0.2	0.4 ± 0.2	0.6 ± 0.2
AA885	**−8.8 ± 0.9**	**−2.9 ± 1.1**	**−2.9 ± 0.2**	**−5.6 ± 0.7**	**−6.1 ± 0.6**	**−3.4 ± 0.2**	**−3.2 ± 0.4**	**3.2 ± 0.5**	**0.5 ± 0.1**
LYS887	0.1 ± 0.1	−1.5 ± 0.2	−2.0 ± 0.7	−2.0±-0.0	−2.8 ± 0.5	−3.3 ± 0.8	2.1 ± 0.0	1.4 ± 0.4	1.3 ± 1.1
GLU915	**−1.7 ± 1.1**	**−0.6 ± 0.4**	**−0.7 ± 0.7**	**−2.1 ± 0.2**	**−1.6 ± 0.3**	**−1.4 ± 0.4**	**0.5 ± 1.2**	**1.0 ± 0.2**	**0.7 ± 0.3**
TRP917	**−7.4 ± 0.8**	**−5.4 ± 1.4**	**−5.5 ± 1.4**	**−10.5 ± 0.9**	**−8.3 ± 1.8**	**−8.1 ± 1.4**	**3.1 ± 0.9**	**2.9 ± 0.4**	**2.6 ± 0.2**
PHE918	**−1.8 ± 0.3**	**−1.6 ± 0.8**	**−1.9 ± 0.4**	**−2.8 ± 0.4**	**−2.4 ± 1.0**	**−2.8 ± 0.4**	**1.0 ± 0.1**	**0.8 ± 0.3**	**0.9 ± 0.3**

The bold values represent the residues with major contribution for the complex interaction.

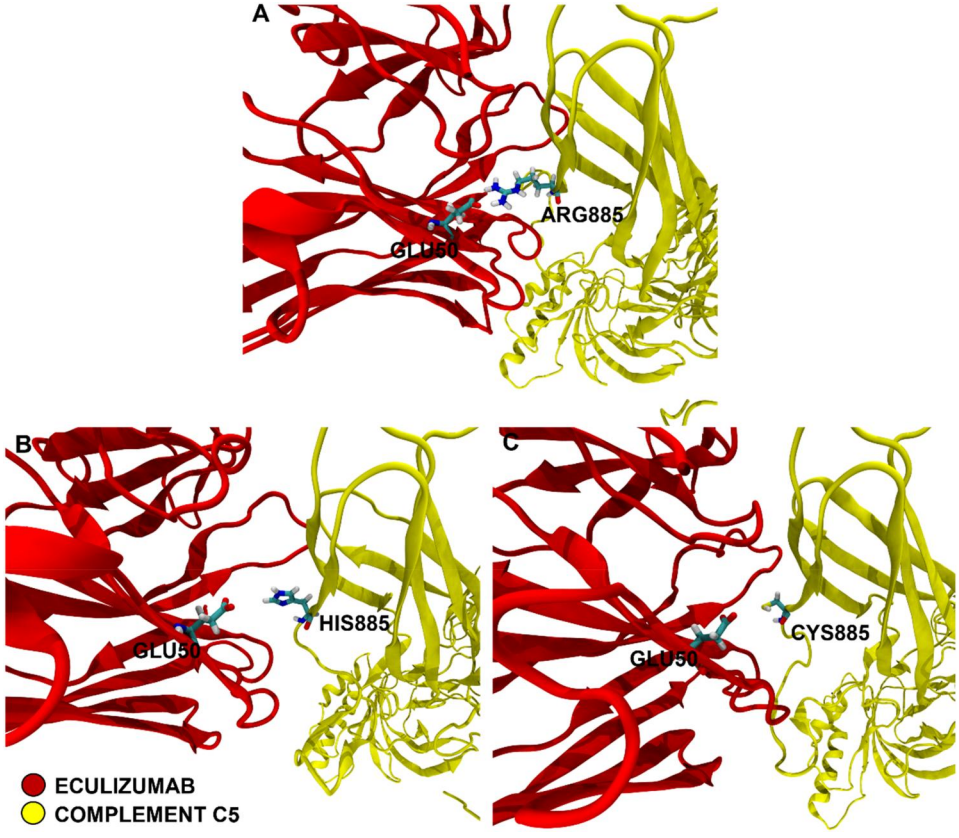

Figure 6. Visual molecular dynamics (VMD) representation of the alignment of the interaction between residue 885 in the wild-type, in the p.Arg^{885}His and in the p.Arg^{885}Cys.

Gln^{854} energy supply turned from −3.5 to −4.0 kcal/mol, p.Arg^{885}Cys variant (more favorable for the polymorphic protein) and turned from −3.5 to −2.7, for p. Arg^{885}His (less favorable).

RMSd and RMSF trajectories

RMSd trajectories can evaluate the deviation of atomic positions. It measures the average distance between the atoms. RMSd values are considered as reliable indicators of variability when applied to very similar proteins, like these polymorphic variations. As can be seen in Supplementary Material (Fig. S1 and Fig. S2), the complex adopts stable conformations after the first 100 ns.

A single mutation on position 885 does not induce a high variation on the stability of the C5 protein (average RMSd C5 4.2 in wt vs. 4.4 Å in mutants). However, an analysis of eculizumab reveals a significantly more drastic change in the average RMSd (6.0 in wt vs. 7.9 and 6.7 Å for the His and Cys variants, respectively). These results suggest that the studied SNP impacts the ability of C5 in stabilizing eculizumab, which comes to adopt a less stable bound conformation in the mutants (Table 4).

Table 4. RMSd and RMSF values.

System	Av. RMSd C5 (Å)	Av. RMSd Eculizumab (Å)	Av. RMSF C5 (Å)
WT	4.2 ± 0.3	6.0 ± 0.7	3.6 ± 1.4
p.Arg^{885}His	4.4 ± 0.2	7.9 ± 0.2	4.0 ± 1.3
p.Arg^{885}Cys	4.4 ± 0.2	6.7 ± 1.0	4.4 ± 1.6

RMSF measures the average deviation of the residues over time from a reference position (Cα), analyzing the portions of the structure that are fluctuating from their mean structure the most. The comparison with the wild type shows that polymorphic variants result in an increase of the amino acid flexibility as the average RMSF shows (3.6 in wt vs. 4.0 and 4.4 Å for the His and Cys variants, respectively; Table 4).

Figure 7A represents the RMSF of the Cα atoms of C5. The results presented are normalized, in the sense that they refer to the average mobility of the Cα on each amino acid residue, indicative of the flexibility of the different backbone positions. The results show that the more flexible regions of the C5 correspond to regions close to the N- and C- terminus. Residues 370–550 exhibit also high flexibility.

Analyzing Figure 7B, we can conclude that the 5 amino acids with major energetic contribution exhibit higher

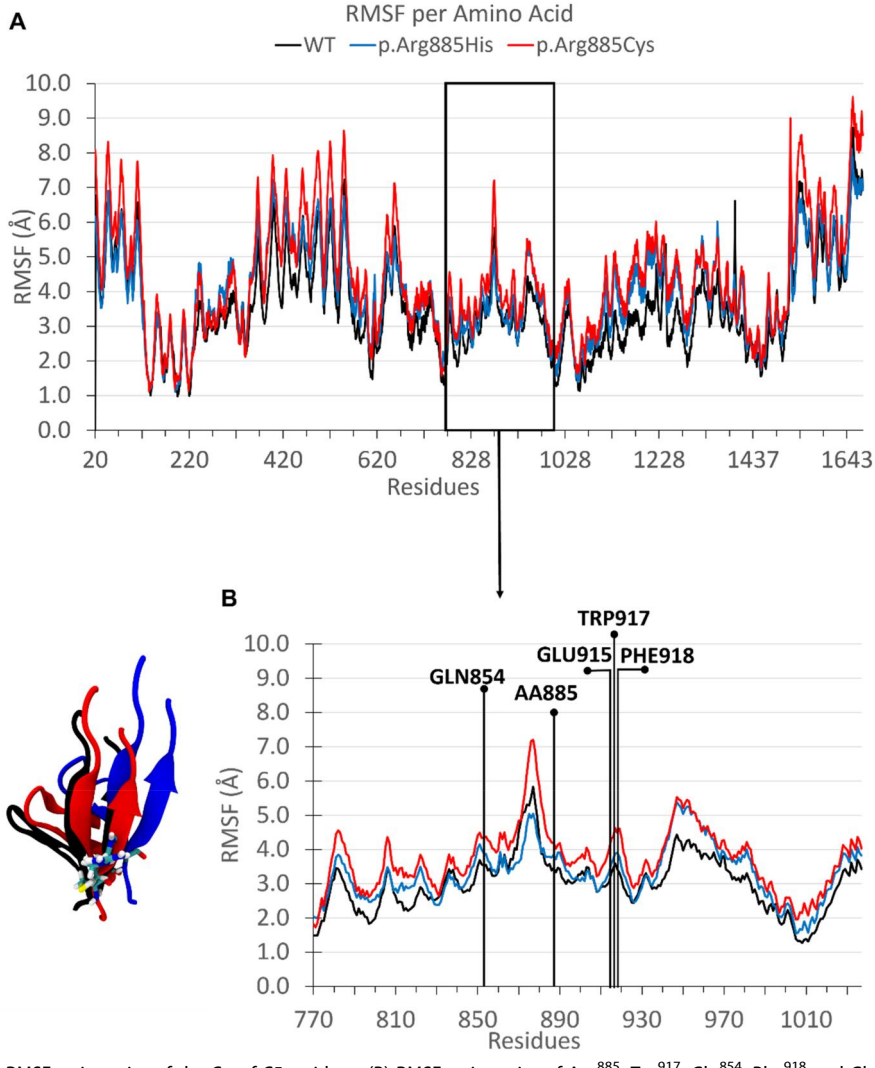

Figure 7. RMSF trajectories (A) RMSF trajectories of the Cα of C5 residues. (B) RMSF trajectories of Arg^{885}, Trp^{917}, Gln^{854}, Phe^{918} and Glu^{915}.

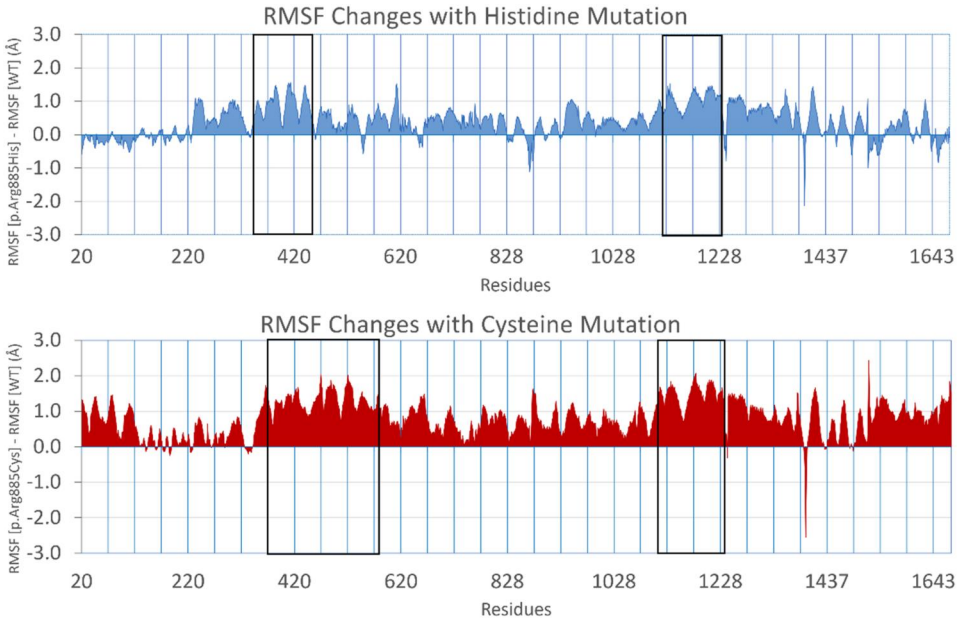

Figure 8. Change in the RMSF for each amino acid residue calculated from the difference between the RMSF of p.Arg^{885}His/p.Arg^{885}Cys and wild-type proteins.

flexibility after Arg^{885} substitution, indicative that their regions become less stabilized by eculizumab.

Figure 8 represents the change in RMSF that takes place with the mutation species, with values calculated from the difference between the RMSF of mutated and wild-type proteins. These representations illustrate the regions of the C5 where the changes in flexibility are more significantly altered. The single amino acid mutation leads to significant conformational changes in the structure of C5. Mutation at 885 position have shown drastically alter the complex interaction. It can be observed that, overall, all residues in C5 exhibit more flexibility when compared to the wild-type. These changes are more pronounced in C- and N-terminal and in the regions bordering the eculizumab epitope zone (residues 350–430 and 1131–1232, for His variant and residues 365–580 and 1150–1230, for Cys variant). The epitope region acquires more flexibility for mutated proteins, but it still does not show as much flexibility as the regions mentioned earlier.

Eculizumab, the first approved treatment for PNH, represented a complete change in the prognosis and outcome of these patients. The poor response of some of them was associated with mutations in C5.

Using computational methodologies, we created a fully integrated analysis of the structural and dynamical behavior of C5 and eculizumab interaction and repeated the simulation with the mutant variants.

The set of results obtained in this study shows that a small change in one single amino acid can significantly impact the structure and flexibility of the enzyme C5. C5-eculizumab interface due to the histidine/cysteine alterations loses affinity.

It is concerning that the lack of effectiveness of the treatment in a disease like PNH can lead to the worsening of clinical, laboratory, and biochemical parameters, as well as the failure to prevent intravascular hemolysis or to provide preventive anti-thrombotic effects. These clinical repercussions can result in an amplification of the overall debilitating symptoms associated with PNH.Several clinical trials are studying other C5 mAb, including crovalimab, which blocks different C5 epitope than eculizumab probably quelling the eculizumab non-responsive c.2654G > A and c.2653C > T mutations. The other C5 mAB approved for the treatment of PNH is ravulizumab, which has 4 amino acid substitutions in the structure of eculizumab, acting as a long-time inhibitor. Ravulizumab interacts with the same epitope as eculizumab, so it does not represent a good choice to replace eculizumab for patients carrying these variants. Also, pegcetacoplan—the first proximal complement C3 inhibitor approved for the treatment of PNH, and iptacopan—the first Factor B inhibitor approved, may represent a good solution for these patients.

Our studies suggest that the poor response to eculizumab in patients with PNH with Arg^{885}His/Cys polymorphisms can be explained by a disturbed functioning of eculizumab blockade, leading to a breakdown in the usual process. This knowledge can be used to design variations in eculizumab that make it less sensitive to alterations in the C5 885 position, contributing to the design of a more universal antibody that could be used with success in patients with different genetic variants at this position.

Ultimately, this assessment can offer a deeper understanding of directed therapies and the development of groundbreaking medicines, highlighting the importance of pharmacogenetics and its role in individualized medicine and pharmacotherapy.

Authors' contributions

Data curation, investigation, methodology, VPP and SFS; Formal analysis, VPP and SFS; Resources, SFS; Supervision, SFS and MV; Validation, VPP and SFS; Visualization, VPP and SFS; Writing original draft preparation, VPP and SFS; Writing, review, and editing, VPP, SFS, MV and CP; All authors have read and agreed to the published version of the manuscript.

Availability of data and material

Available upon reasonable request.

Disclosure statement

The authors report no conflict of interest.

Funding

This work was financially supported with funding from FCT/MCTES (UIDP/50006/2020) through national funds. Some of the calculations were produced with the support of INCD funded by FCT and FEDER under project 01/SAICT/2016 number 022153 and projects CPCA/A00/7140/2020, CPCA/A00/7145/2020, and 2021.09752.CPCA. SFS acknowledges FCT for funding through program 2020.01423.CEECIND.

References

Berman, H. M., Westbrook, J., Feng, Z., Gilliland, G., Bhat, T. N., Weissig, H., Shindyalov, I. N., & Bourne, P. E. (2000). The protein data bank. *Nucleic Acids Research*, *28*(1), 235–242. https://doi.org/10.1093/nar/28.1.235

Bektas, M., Copley-Merriman, C., Khan, S., Sarda, S. P., & Shammo, J. M. (2020). Paroxysmal nocturnal hemoglobinuria: Role of the complement system, pathogenesis, and pathophysiology. *Journal of Managed Care & Specialty Pharmacy*, *26*(12-b Suppl), S3–S8. https://doi.org/10.18553/jmcp.2020.26.12-b.s3

Bessler, M., Mason, P. J., Hillmen, P., Miyata, T., Yamada, N., Takeda, J., Luzzatto, L., & Kinoshita, T. (1994). Paroxysmal nocturnal haemoglobinuria (PNH) is caused by somatic mutations in the PIG-A gene. *The EMBO Journal*, *13*(1), 110–117. https://doi.org/10.1002/j.1460-2075.1994.tb06240.x

Brachet, G., Bourquard, T., Gallay, N., Reiter, E., Gouilleux-Gruart, V., Poupon, A., & Watier, H. (2016). Eculizumab epitope on complement C5: Progress towards a better understanding of the mechanism of action. *Molecular Immunology*, *77*, 126–131. https://doi.org/10.1016/j.molimm.2016.07.016

Brodsky, R. A. (2009). How do *PIG-A* mutant paroxysmal nocturnal hemoglobinuria stem cells achieve clonal dominance? *Expert Review of Hematology*, *2*(4), 353–356. https://doi.org/10.1586/ehm.09.35

Brodsky, R. A. (2014). Paroxysmal nocturnal hemoglobinuria. *Blood*, *124*(18), 2804–2811. https://doi.org/10.1182/blood-2014-02-522128

Brodsky, R. A., Young, N. S., Antonioli, E., Risitano, A. M., Schrezenmeier, H., Schubert, J., Gaya, A., Coyle, L., de Castro, C., Fu, C.-L., Maciejewski, J. P., Bessler, M., Kroon, H.-A., Rother, R. P., & Hillmen, P. (2008). Multicenter phase 3 study of the complement inhibitor eculizumab for the treatment of patients with paroxysmal nocturnal hemoglobinuria. *Blood*, *111*(4), 1840–1847. https://doi.org/10.1182/blood-2007-06-094136

Elzaiat, M., Flatters, D., Sierra-Díaz, D. C., Legois, B., Laissue, P., & Veitia, R. A. (2020). DHH pathogenic variants involved in 46,XY disorders of sex development differentially impact protein self-cleavage and structural conformation. *Human Genetics*, *139*(11), 1455–1470. https://doi.org/10.1007/s00439-020-02189-5

Ferreira, P., Sousa, S. F., Fernandes, P. A., & Ramos, M. J. (2017). Improving the catalytic power of the DszD enzyme for the biodesulfurization of crude oil and derivatives. *Chemistry (Weinheim an der Bergstrasse, Germany)*, *23*(68), 17231–17241. https://doi.org/10.1002/chem.201704057

Fu, R., Li, L., Li, L., Liu, H., Zhang, T., Ding, S., Wang, G., Song, J., Wang, H., Xing, L., Guan, J., & Shao, Z. (2020). Analysis of clinical characteristics of 92 patients with paroxysmal nocturnal hemoglobinuria: A single institution experience in China. *Journal of Clinical Laboratory Analysis*, *34*(1), e23008. https://doi.org/10.1002/jcla.23008

Harder, M. J., Höchsmann, B., Dopler, A., Anliker, M., Weinstock, C., Skerra, A., Simmet, T., Schrezenmeier, H., & Schmidt, C. Q. (2019). Different levels of incomplete terminal pathway inhibition by eculizumab and the clinical response of PNH patients. *Frontiers in Immunology*, *10*, 1639. https://doi.org/10.3389/fimmu.2019.01639

Heeney, M. M., Ormsbee, S. M., Anthony Moody, M., Howard, T. A., DeCastro, C. M., & Ware, R. E. (2003). Increased expression of anti-apoptosis genes in peripheral blood cells from patients with paroxysmal nocturnal hemoglobinuria. *Molecular Genetics and Metabolism*, *78*(4), 291–294. https://doi.org/10.1016/S1096-7192(03)00047-7

Hillmen, P., Muus, P., Röth, A., Elebute, M. O., Risitano, A. M., Schrezenmeier, H., Szer, J., Browne, P., Maciejewski, J. P., Schubert, J., Urbano-Ispizua, A., Castro, C., Socié, G., & Brodsky, R. A. (2013). Long-term safety and efficacy of sustained eculizumab treatment in patients with paroxysmal nocturnal haemoglobinuria. *British Journal of Haematology*, *162*(1), 62–73. https://doi.org/10.1111/bjh.12347

Hillmen, P., Young, N. S., Schubert, J., Brodsky, R. A., Socié, G., Muus, P., Röth, A., Szer, J., Elebute, M. O., Nakamura, R., Browne, P., Risitano, A. M., Hill, A., Schrezenmeier, H., Fu, C.-L., Maciejewski, J., Rollins, S. A., Mojcik, C. F., Rother, R. P., & Luzzatto, L. (2006). The complement inhibitor eculizumab in paroxysmal nocturnal hemoglobinuria. *The New England Journal of Medicine*, *355*(12), 1233–1243. https://doi.org/10.1056/NEJMoa061648

Humphrey, W., Dalke, A., & Schulten, K. (1996). VMD: Visual molecular dynamics. *Journal of Molecular Graphics*, *14*(1), 33–38. https://doi.org/10.1016/0263-7855(96)00018-5

Jore, M. M., Johnson, S., Sheppard, D., Barber, N. M., Li, Y. I., Nunn, M. A., Elmlund, H., & Lea, S. M. (2016). Structural basis for therapeutic inhibition of complement C5. *Nature Structural & Molecular Biology*, *23*(5), 378–386. https://doi.org/10.1038/nsmb.3196

Jumper, J., Evans, R., Pritzel, A., Green, T., Figurnov, M., Ronneberger, O., Tunyasuvunakool, K., Bates, R., Žídek, A., Potapenko, A., Bridgland, A., Meyer, C., Kohl, S. A. A., Ballard, A. J., Cowie, A., Romera-Paredes, B., Nikolov, S., Jain, R., Adler, J., … Hassabis, D. (2021). Highly accurate protein structure prediction with AlphaFold. *Nature*, *596*(7873), 583–589. https://doi.org/10.1038/s41586-021-03819-2

Katsonis, P., Koire, A., Wilson, S. J., Hsu, T.-K., Lua, R. C., Wilkins, A. D., & Lichtarge, O. (2014). Single nucleotide variations: Biological impact and theoretical interpretation. *Protein Science: A Publication of the Protein Society*, *23*(12), 1650–1666. https://doi.org/10.1002/pro.2552

Lapaillerie, D., Charlier, C., Guyonnet-Dupérat, V., Murigneux, E., Fernandes, H. S., Martins, F. G., Magalhães, R. P., Vieira, T. F., Richetta, C., Subra, F., Lebourgeois, S., Charpentier, C., Descamps, D., Visseaux, B., Weigel, P., Favereaux, A., Beauvineau, C., Buron, F., Teulade-Fichou, M.-P., … Parissi, V. (2022). Selection of bis-indolyl pyridines and triphenylamines as new inhibitors of SARS-CoV-2 cellular entry by modulating the spike protein/ACE2 interfaces. *Antimicrobial Agents and Chemotherapy*, *66*(8), e00083-22. https://doi.org/10.1128/aac.00083-22

Magalhães, R. P., Fernandes, H. S., & Sousa, S. F. (2022). The critical role of Asp206 stabilizing residues on the catalytic mechanism of the *Ideonella sakaiensis* PETase. *Catalysis Science & Technology*, *12*(11), 3474–3483. https://doi.org/10.1039/D1CY02271G

Mahtarin, R., Islam, S., Islam, M. J., Ullah, M. O., Ali, M. A., & Halim, M. A. (2022). Structure and dynamics of membrane protein in SARS-CoV-2. *Journal of Biomolecular Structure & Dynamics*, *40*(10), 4725–4738. https://doi.org/10.1080/07391102.2020.1861983

Maier, J. A., Martinez, C., Kasavajhala, K., Wickstrom, L., Hauser, K. E., & Simmerling, C. (2015). ff14SB: Improving the accuracy of protein side chain and backbone parameters from ff99SB. *Journal of Chemical Theory and Computation*, *11*(8), 3696–3713. https://doi.org/10.1021/acs.jctc.5b00255

Martínez-Rosell, G., Giorgino, T., & De Fabritiis, G. (2017). PlayMolecule ProteinPrepare: A web application for protein preparation for molecular dynamics simulations. *Journal of Chemical Information and Modeling*, *57*(7), 1511–1516. https://doi.org/10.1021/acs.jcim.7b00190

Martins, F. G., Melo, A., & Sousa, S. F. (2021). Identification of new potential inhibitors of quorum sensing through a specialized multi-level computational approach. *Molecules (Basel, Switzerland)*, *26*(9), 2600. https://doi.org/10.3390/molecules26092600

Miller, B. R., McGee, T. D., Swails, J. M., Homeyer, N., Gohlke, H., & Roitberg, A. E. (2012). *MMPBSA.py* : An efficient program for end-state free energy calculations. *Journal of Chemical Theory and Computation*, *8*(9), 3314–3321. https://doi.org/10.1021/ct300418h

Mohamed, F. E., Al Sorkhy, M., Ghattas, M. A., Al-Gazali, L., Al-Dirbashi, O., Al-Jasmi, F., & Ali, B. R. (2020). The pharmacological chaperone N-n-butyl-deoxygalactonojirimycin enhances β-galactosidase processing and activity in fibroblasts of a patient with infantile GM1-gangliosidosis. *Human Genetics*, *139*(5), 657–673. https://doi.org/10.1007/s00439-020-02153-3

Muthukumar, V. C. (2023). *Escherichia coli* FtsZ molecular dynamics simulations. *Journal of Biomolecular Structure & Dynamics*, *42*(5), 2653–2666. https://doi.org/10.1080/07391102.2023.2206917

Nishimura, J-I., Yamamoto, M., Hayashi, S., Ohyashiki, K., Ando, K., Brodsky, A. L., Noji, H., Kitamura, K., Eto, T., Takahashi, T., Masuko, M., Matsumoto, T., Wano, Y., Shichishima, T., Shibayama, H., Hase, M., Li, L., Johnson, K., Lazarowski, A., … Kanakura, Y. (2014). Genetic variants in C5 and poor response to eculizumab. *The New England Journal of Medicine*, *370*(7), 632–639. https://doi.org/10.1056/NEJMoa1311084

Onufriev, A., Bashford, D., & Case, D. A. (2004). Exploring protein native states and large-scale conformational changes with a modified generalized born model. *Proteins*, *55*(2), 383–394. https://doi.org/10.1002/prot.20033

Pereira, A. C., Pina, A. F., Sousa, D., Ferreira, D., Santos-Pereira, C., Rodrigues, J. L., Melo, L. D. R., Sales, G., Sousa, S. F., & Rodrigues, L. R. (2022). Identification of novel aptamers targeting cathepsin B-overexpressing prostate cancer cells. *Molecular Systems Design & Engineering*, *7*(6), 637–650. https://doi.org/10.1039/D2ME00022A

Pina, A. F., Sousa, S. F., Azevedo, L., & Carneiro, J. (2022). Non-B DNA conformations analysis through molecular dynamics simulations. *Biochimica Et Biophysica Acta. General Subjects*, *1866*(12), 130252. https://doi.org/10.1016/j.bbagen.2022.130252

Quelhas, D., Carneiro, J., Lopes-Marques, M., Jaeken, J., Martins, E., Rocha, J. F., Teixeira Carla, S. S., Ferreira, C. R., Sousa, S. F., & Azevedo, L. (2021). Assessing the effects of PMM2 variants on protein stability. *Molecular Genetics and Metabolism*, *134*(4), 344–352. https://doi.org/10.1016/j.ymgme.2021.11.002

Risitano, A. M., Marotta, S., Ricci, P., Marano, L., Frieri, C., Cacace, F., Sica, M., Kulasekararaj, A., Calado, R. T., Scheinberg, P., Notaro, R., & Peffault de Latour, R. (2019). Anti-complement treatment for paroxysmal nocturnal hemoglobinuria: Time for proximal complement inhibition? A position paper from the SAAWP of the EBMT. *Frontiers in Immunology*, *10*, 1157. https://doi.org/10.3389/fimmu.2019.01157

Risitano, A. M., Notaro, R., Marando, L., Serio, B., Ranaldi, D., Seneca, E., Ricci, P., Alfinito, F., Camera, A., Gianfaldoni, G., Amendola, A., Boschetti, C., Di Bona, E., Fratellanza, G., Barbano, F., Rodeghiero, F., Zanella, A., Iori, A. P., Selleri, C., Luzzatto, L., & Rotoli, B. (2009). Complement fraction 3 binding on erythrocytes as additional mechanism of disease in paroxysmal nocturnal hemoglobinuria patients treated by eculizumab. *Blood*, *113*(17), 4094–4100. https://doi.org/10.1182/blood-2008-11-189944

Schatz-Jakobsen, J. A., Zhang, Y., Johnson, K., Neill, A., Sheridan, D., & Andersen, G. R. (2016). Structural basis for eculizumab-mediated inhibition of the complement terminal pathway. *Journal of Immunology (Baltimore, Md.: 1950)*, *197*(1), 337–344. https://doi.org/10.4049/jimmunol.1600280

Schmidt, C. Q., Schrezenmeier, H., & Kavanagh, D. (2022). Complement and the prothrombotic state. *Blood*, *139*(13), 1954–1972. https://doi.org/10.1182/blood.2020007206

Schrezenmeier, H., & Höchsmann, B. (2009). Eculizumab opens a new era of treatment for paroxysmal nocturnal hemoglobinuria. *Expert Review of Hematology*, *2*(1), 7–16. https://doi.org/10.1586/17474086.2.1.7

Serrano, C., Teixeira, C. S. S., Cooper, D. N., Carneiro, J., Lopes-Marques, M., Stenson, P. D., Amorim, A., Prata, M. J., Sousa, S. F., & Azevedo, L. (2021). Compensatory epistasis explored by molecular dynamics simulations. *Human Genetics*, *140*(9), 1329–1342. https://doi.org/10.1007/s00439-021-02307-x

Shapovalov, M. V., & Dunbrack, R. L. (2011). A smoothed backbone-dependent rotamer library for proteins derived from adaptive kernel density estimates and regressions. *Structure (London, England: 1993)*, *19*(6), 844–858. https://doi.org/10.1016/j.str.2011.03.019

Takeda, J., Miyata, T., Kawagoe, K., Iida, Y., Endo, Y., Fujita, T., Takahashi, M., Kitani, T., & Kinoshita, T. (1993). Deficiency of the GPI anchor caused by a somatic mutation of the PIG-A gene in paroxysmal nocturnal hemoglobinuria. *Cell*, *73*(4), 703–711. https://doi.org/10.1016/0092-8674(93)90250-t

Varadi, M., Anyango, S., Deshpande, M., Nair, S., Natassia, C., Yordanova, G., Yuan, D., Stroe, O., Wood, G., Laydon, A., Žídek, A., Green, T., Tunyasuvunakool, K., Petersen, S., Jumper, J., Clancy, E., Green, R., Vora, A., Lutfi, M., … Velankar, S. (2022). AlphaFold Protein Structure Database: Massively expanding the structural coverage of protein-sequence space with high-accuracy models. *Nucleic Acids Research*, *50*(D1), D439–D444. https://doi.org/10.1093/nar/gkab1061

Weiser, J., Shenkin, P. S., & Still, W. C. (1999). Approximate atomic surfaces from linear combinations of pairwise overlaps (LCPO). *Journal of Computational Chemistry*, *20*(2), 217–230. https://doi.org/10.1002/(SICI)1096-987X(19990130)20:2<217::AID-JCC4>3.0.CO;2-A